Electrokinetic sorting and collection of fractions for preparative capillary electrophoresis on a chip

Dawid R. Zalewski,* Stefan Schlautmann, Richard B. M. Schasfoort and Han J. G. E. Gardeniers

Received 20th November 2007, Accepted 18th February 2008
First published as an Advance Article on the web 18th March 2008
DOI: 10.1039/b717785b

A microfabricated device capable of selecting and collecting multiple components from a mixture separated by capillary electrophoresis (CE) is described. This collection is automated and can be easily controlled by a set of rules defined by an operator, enabling fast and consistent operation. The device consists of an electrokinetically steered fluidic network that can be divided into three sections: a CE part, a fractions distribution region and a set of storage channels. Sample fractions leave the CE channel and are detected in the interfacial region by fluorescence intensity measurements. If an upcoming peak is detected, separation is withheld and the potentials are reconfigured to force the fraction into one of the collection channels, where they become available for further processing or analysis. The sequence of separation and collection is repeated until all the bands of interest are captured. A mixture of three fluorescent dyes (Rhodamine 6G, Rhodamine B and Fluorescein) was used to demonstrate the principle. The components were repeatedly separated by means of CE and pooled in their respective storage channels. In comparison to previous developments, the system presented in this paper offers automatic collection of all fractions in a single run. Furthermore, it is possible to run the system in a repetitive mode for accumulative pooling if more fractionated sample is required.

Introduction

Since their introduction in the late 1970s/early 1980s,[1,2] capillary electrophoresis and its derivatives have remained the main analytical techniques in biological sciences.[3–5] The potential of the method was demonstrated in the Human Genome Project[6] and today CE serves as the dominant DNA sequencing method. New directions in biological research, such as proteomics, require improved analytical techniques and extensive post-separation sample processing.[7,8] The development of effective procedures for the manipulation and collection of separated fractions is thus of increasing importance.

The first demonstration of fraction collection for capillary electrophoresis was performed by Hjerten and Zhu in 1985[9] on nucleosides, pH markers and IEF ampholytes. In their system, sample was eluted from an open tubular capillary by buffer sheath flow and directed into a number of collection tubes. In the approach of Cohen *et al.*, collection of separated oligonucleotides was achieved by simply inserting the capillary together with an electrode into the tube containing buffer;[10] slab gel electrophoresis was used subsequently to confirm the purity of a collected sample. This method was further extended by applying a field programming technique by Guttman and colleagues,[11] which lowers the separation field during collection, enabling more precise operation.

The disadvantages of manual handling (high voltage hazard; inaccurate timing) were addressed by several groups, which concentrated on process automation. Rose and Jorgenson presented an apparatus that could perform preparative CE with collection into an array of vials by means of a capillary machine moved at pre-programmed times.[12] Lee *et al.* used an autosampler for collection of separated synthetic peptides. A critical aspect of timing was avoided by Huang and Zare who performed direct collection of amino acids onto a rotating drum using a frit structure for elution.[13,14] In the following designs, fractionated proteins were collected onto a rotating circular membrane[15] or onto a moving blotting membrane strip.[16] In both cases, the membranes served as electrical interfaces between the end of the capillary and an electrode, and enabled easy post-processing of collected fractions by sequencing or immunological identification. More recently Minarik and co-workers designed a system for separating DNA fragments using 12 parallel separation capillaries and collection onto a moving microwell gel plate, the position of the fractions was reconstructed after analysis from the electropherograms and collected samples were subjected to PCR and sequencing.[17]

Muller *et al.* constructed a system capable of fully automated detector-triggered fractionation of DNA into a series of machine-switched collection capillaries.[18] A similar concept was presented by Irie and co-workers who performed capillary array electrophoresis and collected the sample in individually addressed vial trays.[19]

The preparative mode of CE was also demonstrated on oligosaccharides using a sheath flow cell detector.[20] This configuration was used in drug analysis in a simple pre-programmed manner.[21]

The concept of a modern micro total analysis system, introduced by A. Manz *et al.* in 1990,[22] together with a

MESA+ Institute for Nanotechnology, Faculty of Science and Technology, University of Twente, P.O Box 217, 7500AE, Enschede, The Netherlands. E-mail: d.r.zalewski@utwente.nl; Tel: +31 53 489 2594

presentation of the first chip-based analytical separation device[23] led to the development of miniaturized electrophoretic systems in 1992.[24,25] Due to the limitations imposed by the nature of electrokinetic control and problems with force balancing at the microscale, most of the focus shifted towards improvement of the microchip CE rather than full system integration. Reports presenting CE as part of an integrated analytical microsystem[26,27] are considered milestones and have drawn the attention of the scientific community.[28]

In the first microchip CE fractionator presented by Effenhauser *et al.*,[29] the separation channel had two exits: one of them was used for collection while the other served as a waste channel. By alternating the applied potentials at predetermined times and closing an electric circuit, fractions could be drawn through either channel. Khandurina *et al.* performed micropreparative separation of DNA fragments in a simple crossed-channels device, employing manual reconfiguration of potentials in order to stop the separation and drive a single fraction into a reservoir for subsequent retrieval.[30] In a device presented by Lin and colleagues, sample fractions were redirected to the side channel at the T-junction and electrically captured downstream by integrated electrodes.[31] Several difficulties concerning the peak dispersion that appeared during manipulation at the junction were later successfully addressed by introducing in-junction electrodes for local shaping of the electric field and thus minimizing undesirable effects.[32] In the fully automated device described by Tulock *et al.*, dispersion was avoided by utilizing a double layer channel system with polycarbonate track-etched membrane serving as fluidic isolation at the junction, but still permitting forced fraction collection after reconfiguration of the steering potentials.[33]

Preparative CE cannot compete with the free-flow electrophoretic techniques if the amount of sample is significant or high-speed operation is required. However, it offers superior resolution, allows the use of capillary fillings and requires no pressure driven flow, so minimizing hardware requirements. A lack of hydraulic components usually implies minimization of dead-volume in the setup and thus reduces the amounts of both sample and analytes needed. A sample fractionated by means of preparative CE can be utilized in numerous ways including, but not limited to, subsequent analysis, *e.g.* amino acid composition, sequencing, MS; or it can be used as a substrate for PCR, functional assays or labelling.[34]

In this paper, we report on the design and operation of a micropreparative CE chip capable of fast fractionation of multiple components from a complex sample. Following the separation, the sample fractions are sorted and stored in individually addressable collection channels, of which the number determines the number of unique collectable components. Real-time, dynamic computer control enables fast and time-stable operation and minimizes samples losses. Timing of the fractionation is triggered by the fluorescence intensity signal resolved by a photomultiplier at the end of the collection channel. Unlike with lab-scale instruments, the device incorporates no mechanical parts to assist the collection; the whole process is controlled electrokinetically. The method described in this report can be utilized as a primary or intermediate step in complex microfluidic systems. The on-a-chip integration of post-fractionation processing overcomes the difficulties with handling very small volumes and avoids the question of sufficiency of the limited amounts of product delivered by a single microscale separation. Lab-scale post-processing requires larger quantities of material. A sufficient amount of a sample can be provided by running the separation/collection procedure multiple times. Repetitive operation causes the accumulation of fractionated sample. As a result, the amount of collected material increases from femtomolar range–a usual product yield achieved in a single run for typical sample concentration–to picomols, a quantity sufficient for most analytical methods.[35–37]

Methods

A schematic drawing of a micropreparative CE chip and a corresponding analyte concentration graph along the channel is shown in Fig. 1. The chip geometry is described in terms of characteristic dimensions: separation channel length–L_S; collection channel length–L_C; and, for double-T injection, initial analyte plug width–$2h$. The half-width w of an analyte band is defined by its standard deviation σ and equals: 3σ and $h + 3\sigma$ for Gaussian and boxcar plug profiles respectively. It is also assumed that a method exists for manipulating the electric field independently in the separation and collection channels, *i.e.* performing separation while withholding collection and vice versa. This method will be discussed later.

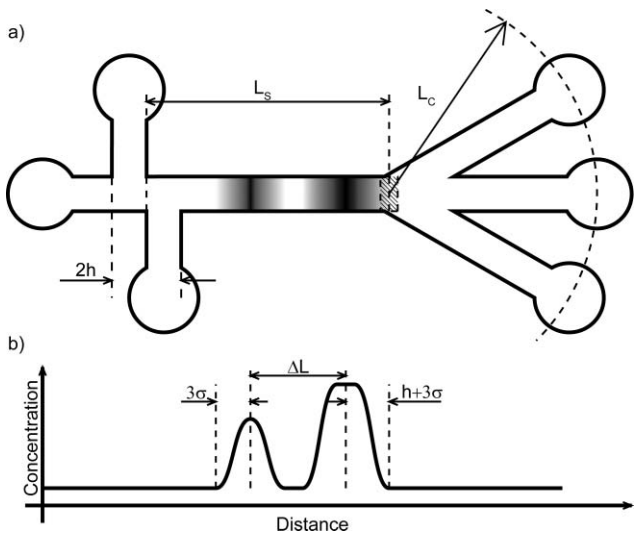

Fig. 1 Schematic representation of a micropreparative CE chip device: (a) characteristic dimensions; (b) concentration profile of two plugs.

General system considerations

Scaling laws of miniaturization,[38] *i.e.* reduction of distances and decrease of duration of processes as compared to traditional systems, require more precise timing and higher spatial resolution of sample handling. Limits imposed by these requirements can be defined by a minimum operating frequency f_S needed for an accurate spatial manipulation of fractions such that:

$$f_S > \frac{u_{max}}{\min(2w_{min}, \Delta L_{min})} \quad (1)$$

where u_{max} is the maximum average velocity of a sample, $2w_{min}$ the minimum sample zone width and ΔL_{min} the minimum

distance between adjacent plugs. The feasibility of manipulation is usually determined by the full separation of the fractions:

$$\Delta L_{\min} > 2 \cdot w_{\min} \tag{2}$$

For practical use in micropreparative CE systems, eqn (1) combined with the assumption (2) can be written as:

$$f_S t_{D1} > \frac{1}{\gamma} \frac{L_S}{\sigma_1} \tag{3}$$

where t_{D1} denotes the time needed for the most mobile fraction to reach the interface between the separation and collection parts, σ_1^2 is the variance of the fraction at time t_{D1}, L_S is a length of the separation channel and γ is a parameter describing the desired spatial separation, *e.g.* for peaks with Gaussian concentration profiles it can be any number between 4 and 6 depending on the criterion used.

Since f_S usually depends on the hardware used and is limited by the computing speed and the response times of detectors and actuators, it cannot easily be altered. Thus, having fixed f_S, other parameters such as buffer composition, electric field strength and chip geometry need to be adjusted to obey the condition (3).

Information about the exact locations of fractions at any instant during separation and collection is an important prerequisite for the successful operation of micropreparative CE. In passive systems,[29–31] such information is obtained from preliminary separations and an assumption is then made that the separation conditions instability over time does not result in positional errors Δs that lead to erroneous manipulation and sample misplacement, thus:

$$\Delta s << \frac{u_{\max}}{f_S} \tag{4}$$

Active systems[33] collect their data during the separation through detection sites located at the channel and process it in order to reconstruct real-time information about the state of the process. In the simplest configuration, only one sensor is required at the interface between the separation and collection parts of the system. Usually a detector provides only data about the concentration profile of a passing band transformed by the detector's function. Based on this and given the position of an analyte at time t_0, the distance from an injection point to a detector L_S and the electric field strength, the fraction properties such as mobility and diffusivity and its exact position can be calculated. Therefore on the assumptions that: (a) external physical conditions are stable during a single run; (b) the electric field can be fully controlled and defined for any instant; and (c) the system meets the minimum f_S criterion; then this information can be later used for guiding the sample into an appropriate collection channel. Usually, active systems are able to deliver better results than passive devices and surpass the latter in adaptability. However, active systems are more complex than passive devices and require longer development times.

Model of operation

The performance of the device is strongly affected by the model of operation used internally to reconstruct sample parameters (mobility, diffusivity) and values of system variables (the operation's progress, positions of the fractions). If the conditions of time stability and definability of the potential distribution during the operation are met, the micropreparative CE device can be considered as a system that operates at three distinguishable electric field strengths: E_S–the electric field of separation, that is the field applied over separation channel length during the separation phase; E_C–the electric field of collection, that is the field applied over the collection channel length during the collection phase and acting on the currently collected fraction, E_B–the electric field applied over the separation channel during the collection phase and acting on the fractions that have not yet been collected. The electric field function of i-th sample (that is the sample with the i-th greatest total mobility) is then given by:

$$\begin{aligned} E_i(t) = {} & E_S H(t) + \\ & (E_S - E_B) \sum_{j=1}^{i-1} \left[H(t - t_{Cj}) - H(t - t_{Dj}) \right] + \\ & (E_C - E_S) H(t - t_{Di}) - E_C H(t - t_{Ci}) \end{aligned} \tag{5}$$

where t_{Di}, t_{Dj} is the time at which an i-th (or j-th) sample reaches the interface between the separation and collection parts of the system; t_{Ci}, t_{Cj}–the time at which i-th (or j-th) sample reaches its final collection position and $H(\tau)$ is the Heaviside function. The times t_C and t_D can be obtained by applying following equations:

$$t_{Di} = \left[\frac{\mu_1}{\mu_i} + \frac{\alpha}{\beta}(1-\eta) \sum_{j=1}^{i-1} \frac{\mu_1}{\mu_j} \right] t_{D1} \tag{6}$$

$$t_{Ci} = \left[\frac{\mu_1}{\mu_i} \left(1 + \frac{\alpha}{\beta} \right) + \frac{\alpha}{\beta}(1-\eta) \sum_{j=1}^{i-1} \frac{\mu_1}{\mu_j} \right] t_{D1} \tag{7}$$

where symbols α, β and η are defined as:

$$\begin{cases} L_S = L \\ L_C = \alpha L \\ E_S = E \\ E_C = \beta E \\ E_B = \eta E \end{cases} \tag{8}$$

and:

$$t_{D1} = \frac{L_S}{\mu_1 E_S} \tag{9}$$

The position of a sample at any instant can be determined by integrating eqn (5) over time and then multiplying the result by sample mobility:

$$x_i(t) = \mu_i \int_0^t E_i(\tau) \mathrm{d}\tau \tag{10}$$

The result of the integration is presented in Appendix A. The concentration profile of the sample is then given for Gaussian (11) and boxcar (12) plugs as:

$$C_i(x,t) = \frac{C_{0i}}{\sigma_i \sqrt{2\pi}} \exp\left(- \frac{\left(x - \mu_i \int_0^t E_i(\tau) \mathrm{d}\tau \right)^2}{2\sigma_i^2} \right) \tag{11}$$

$$C_i(x,t)=\frac{C_{0i}}{2}\left[erf\left(\frac{h-x+\mu_i\int_0^t E_i(\tau)\mathrm{d}\tau}{2\sqrt{D_i t}}\right)+erf\left(\frac{h+x-\mu_i\int_0^t E_i(\tau)\mathrm{d}\tau}{2\sqrt{D_i t}}\right)\right] \quad (12)$$

where: $\sigma_i^2 = \sigma_{\mathrm{inj}}^2 + 2D_i t$ and σ_{inj}^2 denotes the initial injection variance of a plug.

It can be further related to the response of a detector by convolving (11) or (12) with a detector response function.[39] Applying the model equations to data obtained from detectors and known system parameters produces information needed for proper, dynamic control of the collection process.

Performance measures

Many well established measures of the quality of separation exist such as resolution, plate height or plate number.[39] Despite their widespread use they provide limited feedback when applied to preparative techniques, because they either depend on spatial separation as such, which in fraction collection is defined by system geometry, or because the quantities they define do not contain any information about the effectiveness of the collection process. As a consequence, the number of collectable fractions is introduced as an important performance metric.

Number of collectable fractions

The collection of two adjacent fractions is limited by the system's ability to recognize them at the interface between the separation and collection parts and to handle them independently. If the system operates at the minimum frequency f_S, this requirement can be easily met when there is no overlapping of the fractions:

$$x_i(t)-x_{i+1}(t)>\gamma\frac{\sigma_i(t)+\sigma_{i+1}(t)}{2} \quad (13)$$

Here γ is an arbitrararily chosen number describing the quality of separation, *e.g.* for Gaussian plugs $\gamma = 6$ defines a full baseline separation. On the assumption that the diffusivity of the analyte components is constant over the whole set, this general condition can be rewritten as:

$$\frac{\mu_i-\mu_{i+1}}{\mu_i}L_S>\gamma\sqrt{\sigma_{\mathrm{inj}}^2+2Dt_{\mathrm{D}i}} \quad (14)$$

$$\frac{\mu_i-\mu_{i+1}}{\mu_i}L_S>\gamma\left(\frac{\sigma_{\mathrm{inj}}}{\sqrt{3}}+\sqrt{2Dt_{\mathrm{D}i}}\right) \quad (15)$$

for Gaussian (14) and boxcar (15) injection profiles, respectively. The right side of eqn (15) is the result of taking the integration limits for a concentration profile function consistent with those for Gaussian plugs, *i.e.* such that for $\gamma = 6$, (15) defines the full baseline separation. It is easy to show that, for any instant at least 99.7% of mass fraction of a boxcar concentration profile plug is contained within the range expressed below:

$$(x_i - (h + 3\sigma_{\mathrm{D}}), x_i + (h + 3\sigma_{\mathrm{D}})) \quad (16)$$

For calculation of the number of collectable fractions, a sample mixture that contains a limited number of components with equal diffusivities and mobilities μ_i that form an arithmetic series is defined as:

$$\begin{aligned}\mu_i-\mu_{i+1}&=const=\Delta\mu\\ \mu_i&=\mu_1-(i-1)\Delta\mu\end{aligned} \quad (17)$$

By using the definition of the dimensions (8) and applying (17) to (14) and (15), the collectability criterion can be reduced to a non-dimensional form given for Gaussian (18) and boxcar (19) injection profiles as follows:

$$\frac{\varphi}{1-(i-1)\varphi}\sqrt{\frac{Pe^*}{\chi Pe^*+2\zeta(i)}}>\gamma \quad (18)$$

$$\frac{\varphi}{1-(i-1)\varphi}\frac{\sqrt{Pe^*}}{\sqrt{\frac{\chi Pe^*}{3}}+\sqrt{2\zeta(i)}}>\gamma \quad (19)$$

The $\zeta(i)$ is a function obtained from (6) and (17) that describes the relation between the collection time of the first fraction t_{D1} and i-th fraction $t_{\mathrm{D}i}$:

$$t_{\mathrm{D}i}=t_{\mathrm{D1}}\zeta(i) \quad (20)$$

It is defined as:

$$\zeta(i)=\zeta(i,\varphi,\alpha,\beta,\eta)=\begin{cases}1 & i=1\\ \dfrac{1}{1-(i-1)\varphi}+\dfrac{\alpha}{\beta}(1-\eta)\displaystyle\sum_{j=0}^{i-2}\frac{1}{1-j\varphi} & i>1\end{cases} \quad (21)$$

The dimensionless parameters used in (18) and (19) are: φ–dependent on the analyte mixture composition, Pe^*–Péclet number related to the separation path length and χ–a number characterizing the initial plug variance related to the square of separation path length.

$$\begin{cases}\varphi=\dfrac{\Delta\mu}{\mu_1}\\ Pe^*=\dfrac{\mu_1 EL}{D}\\ \chi=\dfrac{\sigma_{\mathrm{inj}}^2}{L^2}\end{cases} \quad (22)$$

Eqn (19) can be rewritten in a form closely resembling that of (18):

$$\frac{\varphi}{1-(i-1)\varphi}\Lambda(\vartheta)\sqrt{\frac{Pe^*}{\chi Pe^*+2\zeta(i)}}>\gamma \quad (23)$$

where $\Lambda(\vartheta)$ is given by:

$$\begin{cases}\Lambda(\vartheta)=\dfrac{\sqrt{3+\vartheta}}{1+\sqrt{\vartheta}}\\ \vartheta=\dfrac{6\zeta(i)}{\chi Pe^*}\end{cases} \quad (24)$$

It can be seen that for large ϑ (*i.e.* long time, small initial peak widths, high diffusion coefficient, long separation channels, thus everything that makes the diffusional dispersion significant)

$\Lambda(\vartheta)$ tends to 1 and (19) is reduced to the form given for Gaussian plugs in eqn (18). In further analysis, eqn (23) will be used as the main collectability criterion with $\Lambda(\vartheta) = 1$ for Gaussian plugs and $\Lambda(\vartheta)$ defined by (24) for boxcar plugs.

The number of theoretically collectable fractions can be obtained by calculating the first positive root i of a function:

$$f\left(i,\varphi,Pe^*,\chi,\alpha,\beta,\eta\right) = \frac{\varphi}{1-(i-1)\varphi}\Lambda(\vartheta)\sqrt{\frac{Pe^*}{\chi Pe^* + 2\zeta(i)}} - \gamma \quad (25)$$

Solving this problem analytically is not trivial, but the solution can also be obtained by a numerical search for the smallest n such that:

$$n \in N : \left(f\left(n,\varphi,Pe^*,\chi,\alpha,\beta,\eta\right) > 0\right) \wedge \left(f\left(n+1,\varphi,Pe^*,\chi,\alpha,\beta,\eta\right) \le 0\right) \quad (26)$$

If found, n denotes the maximum number of theoretically collectable fractions from a sample mixture with properties defined in (17).

In Fig. 2, the results of the calculation of the theoretical number of collectable components for a boxcar injection profile are shown. Parameters used in calculations were: $\alpha/\beta = 1/1.5$, $\eta = 0$, and additionally in Fig. 2a $\chi = ((28.9 \times 10^{-6})/(2 \times 10^{-2}))^2$ (plug length $2h$ = 100 μm). It is clear that for large Pe^*, the number of collectable fractions is limited only by the analyte composition, *i.e.* all the fractions can be collected, whereas for lower Pe^* values the collection is diffusion-limited, the transition region width depends on the value of ϕ. It can be also noted that increasing the value of χ greatly decreases the number of collectable components for a given Pe^*. This effect is most noticeable in complex samples. It is an important design consideration as, depending on other parameters and needs, it has to be decided whether to increase throughput by maximizing the injection volume or to focus on the system flexibility and its possible application in multicomponent sample analysis. Additionally, it must be noted that although the number of theoretically collectible components is relatively large, in practice it is limited by the number of collection channels. To accommodate for a larger quantity of fractions to be collected, the chip design must incorporate a corresponding number of supplementary collection channels.

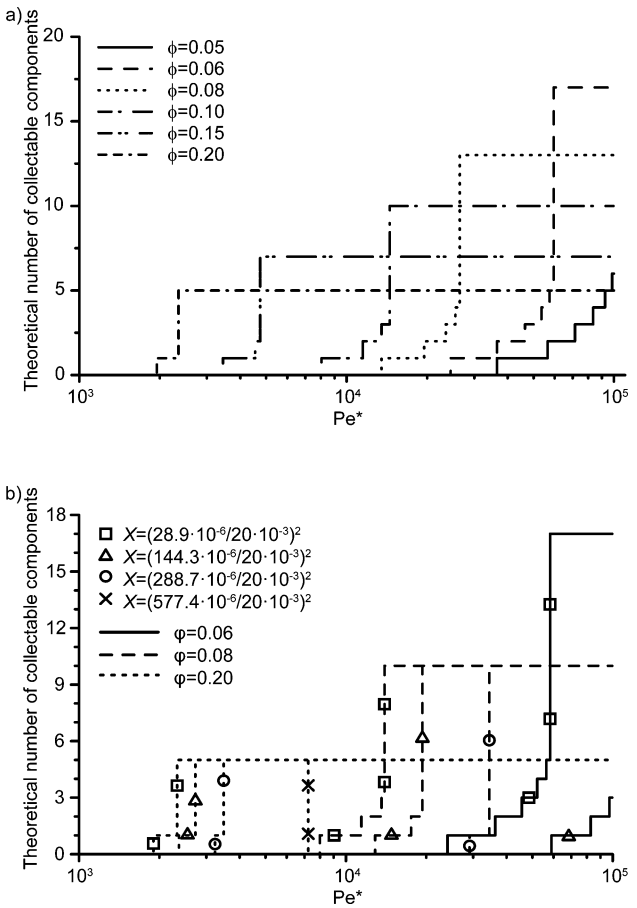

Fig. 2 Graphs of calculated theoretical number of collectable components for: (a) varying φ and (b) varying χ; for boxcar injection concentration profile.

Experimental

Materials

Rhodamine B, rhodamine 6G, fluorescein, 2-(*N*-morpholino)ethanesulfonic acid (MES), histidine, NaOH and isopropyl alcohol (IPA) were obtained from Sigma–Aldrich. Stock solutions of 10 mg mL^{-1} of rhodamine B, rhodamine 6G, 6 mg mL^{-1} of fluorescein, 100 mM MES and histidine were prepared in demineralized water. Prior to experiments, stock solutions were used to prepare 20 mM MES–histidine buffer at pH 6.35 and 0.1 mM rhodamine B, rhodamine 6G, fluorescein in 20 mM MES–histidine sample solution. All mixtures were filtered with 0.22 μm membrane filters and degassed in vacuum for 30 minutes before transferring onto a chip.

Device fabrication

A photograph of the chip is shown in Fig. 3. The fluidic network was filled with a red dye for visualization. The conductivity detector, of which electrodes are marked with symbol 'D' on the picture, was not used in experiments.

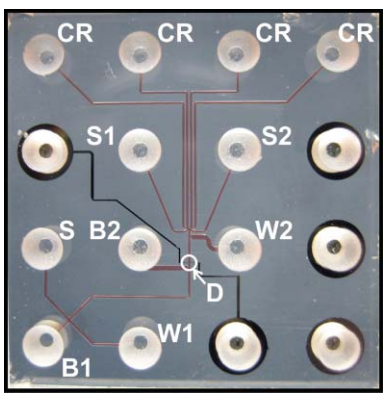

Fig. 3 Photograph of a chip with visible fluidic network.

The chip consists of two bonded 1.1 mm thick borosilicate glass plates. The top plate contains the fluidic channels as well as reservoir openings. To create the fluidic channels, a 10 nm

chromium adhesion layer followed by a 140 nm gold layer was sputtered on a 100 mm glass wafer (Schott Borofloat 33). The Cr/Au layer is resistant to hydrofluoric acid and acts as a mask during wet-etching of the channels. The transfer of the fluidic network design into the Cr/Au mask was carried out by photolithography with Olin 907/17 photoresist, followed by removal of gold and chromium in the exposed areas by wet-etching. Subsequently, a 10% solution of hydrofluoric acid was used to etch 10 μm deep channels into the glass. The reservoir openings were fabricated by micro-powderblasting with 29 μm Al_2O_3 particles through a patterned 100 μm thick polymer photoresist foil, as described by Wensink *et al.*[40] After stripping of the photoresist layers in acetone and removal of the Cr/Au mask by wet-etching, the top and bottom glass wafers were cleaned in 100% HNO_3 for 15 min, followed by rinsing and dry spinning. Next the wafers were brought into close contact to obtain a pre-bond. Light pressure was applied to spread the pre-bonded area across the entire wafer. Irreversible bonding was achieved by annealing at 600 °C for one hour. Finally, the bonded wafer stack was diced into separate 20 mm x 20 mm chip devices.

Instrumentation

A custom-made holder was used to provide electrical and fluidic connections to the chip. Three high-voltage, four-channels power supplies (CU 411, IBIS Technologies, Hengelo, the Netherlands) served as voltage sources. The fluorescence intensity measured by a photomultiplier tube at the point marked with symbol 'D' in Fig. 3 was used for fractions detection. The amplified detector signal was acquired with a multimeter (Agilent 34401A). Utilization of a digital multimeter with an independent detector allows for use of other detection methods employed commonly in CE. The instruments were controlled by a native Windows™ application, written in-house, with a time resolution of at least 40 ms. An inverted microscope (Olympus IX51) equipped with a mercury burner, fluorescent filter set (XF57, Omega Optical, USA) and a 36 bit colour CCD camera (ColorView II, Olympus) controlled by Analysis software package (Olympus Soft Imaging Solutions) was used for visualization.

Chip operation

For a description of the operation of fractionation, we refer to the symbols in Fig. 3.

The operation starts after submitting a steering script that contains injection and separation fields, injection time, sheath flow magnitudes, collection velocities and a set of fractions selected for collection, all to the control application. First, a quick flushing procedure is performed by forcing buffer flow between B1 and W2, then between B2 and CR, and finally between S1, S2 and CR reservoirs. Subsequently a buffer is allowed to flow from B1 to W2 under pre-defined separation conditions and the data for establishing background fluorescence magnitude is collected. The separation starts with an injection of a sample into the separation channel by applying voltages to sample reservoir (S) and waste (W1). Next, the voltages are switched to establish a separation field by applying a potential difference between the buffer source (B1) and the waste (W2). On the decision of an operator, a pre-fractionation run can be made at this point. This step is completely optional and meant only for choosing the fractions to be collected or checking the separation conditions. If the pre-fractionation is omitted, the operator must know which fractions should be collected in advance or let the system collect the components in arrival order. The pre-fractionation is achieved by allowing all the fractions to go to the waste (W2) passing the detector; an electropherogram recorded during this step and mobilities calculated from it are used in the subsequent runs as a base for fractionation. Alternatively, a standard separation/collection cycle is performed. The collection procedure is triggered by threshholding the detector signal. The separation field is kept until a fraction passes the detection point, next the potentials are reconfigured; separation is withheld and in the case of a fraction pre-selected for waste, the voltages are applied to buffer source (B2) and waste (W2) forcing the sample to enter waste reservoir W2. In the case of collection, migration of a sample is forced between B2 and one of the collection channels (CR). Additionally, a sheath flow from S1 and S2 is switched on by applying appropriate voltages, resulting in electrokinetic focusing of a sample to assist the collection and prevent diffusional cross-contamination of the collection channels. During the collection, an electric field distribution is established, based on electrophoretic mobility of a fraction calculated from a recorded migration time and a desired collection velocity value provided by an operator. In the case of accumulative collection, when fractions already reside in the storage channels, at least one of these channels must be used as a waste sink for a buffer volume preceding the sample being collected. Directing unwanted buffer to the waste channel prevents dilution of the pooled fractions and possible contamination.

Results and discussion

Fraction collection and accumulation

Three fluorescent standards were used to demonstrate collection of a CE separated sample. Fig. 4a shows a composite image of collection channels after a series of 30 consecutive full separation/collection cycles. The device was operated in an automated fashion with only three field strengths (E_S = 750 V cm^{-1}, E_C = 550 V cm^{-1}, E_{inj} = 1250 V cm^{-1}) and the injection time (t_{inj} = 3 s) defined in a steering script. Three channels containing separated sample fractions are visible; there is also a waste channel, which cannot be clearly distinguished due to very low fluorescent dyes concentration within it. Fluorescence intensity profiles measured along all four collection channels are shown in Fig. 4b. Gaussian-like peaks can be observed in the channels used for collection, with broader and lower peaks to the right due to their longer residence in the channels and thus greater diffusional dispersion. The magnitude of measured fluorescence of the waste channel is significantly lower as compared to the other channels; a slight increase of intensity can, however, be noticed as the position along the channel progresses. The purity of the collected fractions and the nature of the contamination in the waste channel were assessed by mapping the fluorescence image into the sRGB colour space. Fig. 4c shows the intensity plots of the primary colours of the sRGB colour space (red,

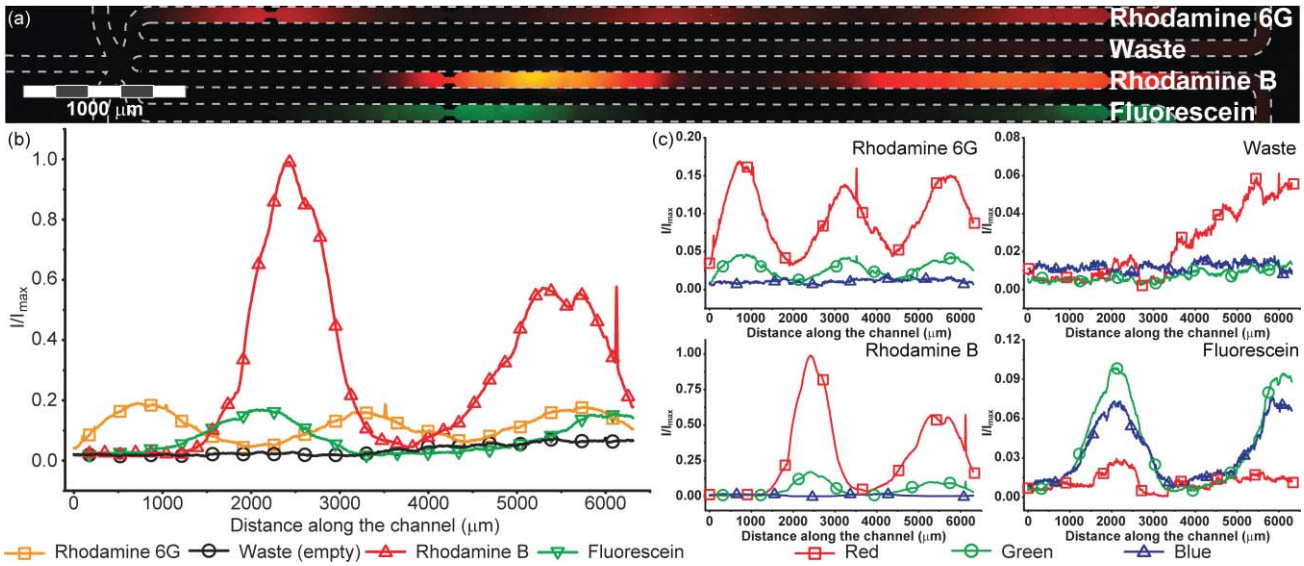

Fig. 4 Results of separation/collection of fluorescent standards; (a) composite fluorescence image of collection channels with stored fractions (brightness has been enhanced for visualization); (b) fluorescence intensity graphs along the channels; (c) intensity profiles of primary colours in the sRGB colour space along the channels.

green, blue). The differences between the plots of the fractions are clearly visible. The most pronounced colour component in rhodamine B and rhodamine 6G, red, is not noticeable in fluorescein; also blue, plainly visible in fluorescein, is virtually absent from both rhodamines. The fluorescence observed in the waste channel is most likely a result of contamination by either rhodamine B or rhodamine 6G; this conclusion can be drawn from the sRGB intensity profiles and the location of the impurity.

The cross-contamination between adjacent channels, seen in the waste channel, although very small, is almost impossible to avoid; this is due to the lack of techniques for incorporating adjustable mechanical barriers into an electrokinetically operated device, drag force acting on a steady fluid when in contact with a moving stream and penetration of the electric field into floating side channels at the crossings. The results of the final phenomena can be minimized to some extent during the collection by utilizing electrokinetic focusing of the sample stream, as shown in Fig. 5. The unwanted spreading of fractions demonstrated in Fig. 5a,b is easily avoided as shown in Fig. 5c,d; the fill coefficient of the focusing (*i.e.* a fraction of the stream width occupied by a sample) was 85%. A visible, non-significant flow of parts of the fractions to the left-sided adjacent collection channels is caused by an unbalanced leak from the waste channel W2.

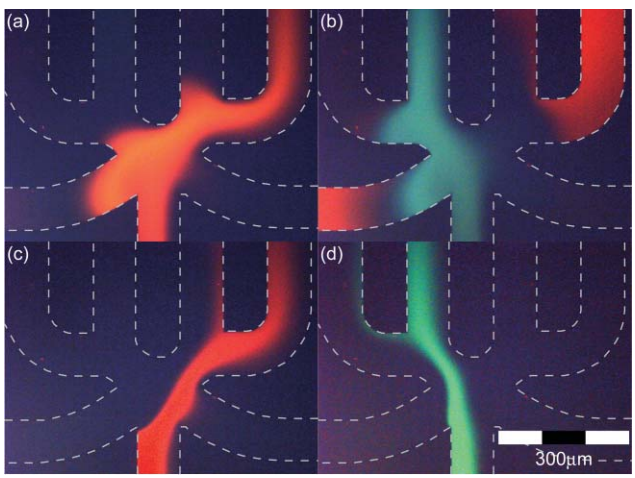

Fig. 5 Fractions guiding: rhodamine B entering the 4th collection channel (a) without electrokinetic focusing, (c) with electrokinetic focusing; fluorescein entering the 2nd collection channel after rhodamine B has been stored: (b) without electrokinetic focusing, (d) with electrokinetic focusing.

Overlapping fractions

In some scenarios, it may be difficult to achieve full electrophoretic separation of adjacent fractions. However, it is still advantageous to collect them individually even if some contamination is unavoidable. Those situations can be addressed by a technique of forced electrokinetic splitting of overlapping components. For performing forced division, the fractions must be positioned at a crossing (or a t-junction) in such a way that the minimum between the peaks is located exactly in the middle of a junction. At this point, the potentials are reconfigured so that the flow is forced from the side channel into the channel that contains the sample. This results in fractions being pushed aside and forced to separate. Such a scheme may be also useful in electrokinetic column coupling, *e.g.* in the case of blood analysis by CE, where a low-abundant peak of Li^+ is cut off from a large concentration Na^+ zone.[41] To demonstrate application of this technique in preparative CE, a separation of a mixture of rhodamine B–rhodamine 6G was performed. The injection plug width was 500 μm and the separation and collection fields were both lowered to around 375 V cm^{-1}; performing separation under these conditions resulted in overlapping of the rhodamine fractions at the arrival to the detection point. The fluorescence intensity profiles taken during the consecutive steps of artificial splitting are show in Fig. 6a,b,c. A clear division of the peaks can

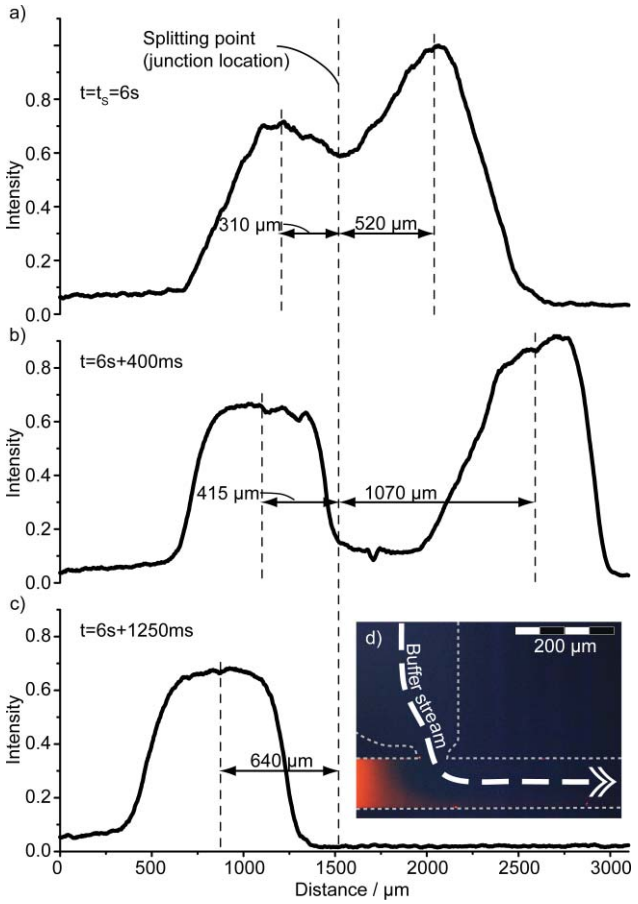

Fig. 6 Forced splitting of overlapping fractions of rhodamine B and rhodamine 6G. Fluorescence intensity profiles taken after (a) 0 ms, (b) 400 ms, (c) 1250 ms from the beginning of operation; (d) fluorescence image of the front of rhodamine B peak at the junction.

be seen as well as distortion of their shapes due to the applied conditions. A microscopic fluorescent picture of rhodamine B fraction front at the junction taken around 400 ms after splitting is shown in Fig. 6d.

Time stability and repeatability

The reproducibility of the separation/collection process was tested in two series of experiments with 30 minutes in between. Each series consisted of ten full runs separated by 30 second breaks; six middle experiments in each series were utilized for measurements. The positions and standard deviations of the fractions were determined by least-square fitting to the Gaussian function (11) of the intensity profiles computed from the fluorescence images taken directly after a collection of each fraction. As seen in Fig. 7, the reproducibility of collection between the series and the runs is very good. The fractions were pre-programmed to stop at the distance of 2000 µm (rhodamine B, 0.33 of the length of collection channels) and 1500 µm (fluorescein, 0.25 of the length of collection channel). Misplacement of the samples falls into the theoretical limits defined by the operating frequency (4); with $u_{max} = 3100$ µm s^{-1} and $f_S = 25$ Hz the maximum theoretical positional error is $\Delta s =$ 124 µm, that is 0.021 of the length of collection channels.

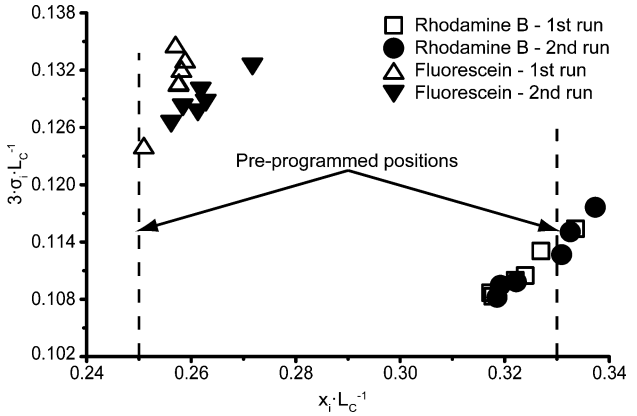

Fig. 7 Reproducibility of the operation. Positions in collection channels *versus* half-widths of peaks directly after storing for two consecutive series are plotted.

Conclusions

A method was proposed for performing micro-preparative CE on a chip that allows for the accumulative pooling of all fractions. Furthermore, the model of operation and a set of parameters were introduced, resulting in optimization guidelines and considerations for the setup and chip design.

The system based on the described principles was built and microfluidic preparative capillary electrophoresis was successfully performed in an automated fashion on a sample mixture. The decoupling of separation and collection processes, realized by individual addressing of both sections of the chip, enabled collection of all the components in a single run and pooling of identical fractions in tight series. Also, the application of the electrokinetic focusing for prevention of cross-contamination between adjacent channels in fluidic manifolds was demonstrated, with very good results. By utilizing active, real-time computer control of the operation excellent reproducibility and time stability of the operation was achieved. It was also shown that automatic control combined with a proper fluidic network design allows for 'mechanical' splitting of overlapping fractions separated by CE. The techniques, described in this paper, for fast and precise electrokinetic manipulation of individual sample zones in aqueous solution may also be applicable in other systems, *e.g.* multidimensional separation, accurate sample delivery and weighting for labelling or reaction studies, positioning for local surface-dependent studies or localized measurements.

Appendix A

The result of calculating the integral (10):

$$x_i(t) = \mu_i \left\{ \begin{array}{l} E_S t H(t) + \\ (E_S - E_B) \sum_{j=1}^{i-1} \left[(t - t_{Cj}) H(t - t_{Cj}) - (t - t_{Dj}) H(t - t_{Dj}) \right] + \\ (E_C - E_S)(t - t_{Di}) H(t - t_{Di}) - E_C (t - t_{Ci}) H(t - t_{Ci}) \end{array} \right\} \quad (27)$$

Notes and references

1 F. E. P. Mikkers, F. M. Everaerts and T. Verheggen, *J. Chromatogr.*, 1979, **169**, 11–20.

2 J. W. Jorgenson and K. D. Lukacs, *Anal. Chem.*, 1981, **53**, 1298–1302.
3 Y. F. Huang, C. C. Huang, C. C. Hu and H. T. Chang, *Electrophoresis*, 2006, **27**, 3503–3522.
4 J. Kraly, M. A. Fazal, R. M. Schoenherr, R. Bonn, M. M. Harwood, E. Turner, M. Jones and N. J. Dovichi, *Anal. Chem.*, 2006, **78**, 4097–4110.
5 B. F. Liu, B. Xu, G. Zhang, W. Du and Q. M. Luo, *J. Chromatogr., A*, 2006, **1106**, 19–28.
6 N. J. Dovichi and J. Z. Zhang, *Angew. Chem., Int. Ed.*, 2000, **39**, 4463–4468.
7 J. I. Haleem, *Electrophoresis*, 2001, **22**, 3629–3638.
8 W. S. Hancock, S. L. Wu and P. Shieh, *Proteomics*, 2002, **2**, 352–359.
9 S. Hjerten and M.-D. Zhu, *J. Chromatogr., A*, 1985, **327**, 157–164.
10 A. S. Cohen, D. R. Najarian, A. Paulus, A. Guttman, J. A. Smith and B. L. Karger, *Proc. Natl. Acad. Sci. U. S. A.*, 1988, **85**, 9660–9663.
11 A. Guttman, A. S. Cohen, D. N. Heiger and B. L. Karger, *Anal. Chem.*, 1990, **62**, 137–141.
12 D. J. Rose and J. W. Jorgenson, *J. Chromatogr., A*, 1988, **438**, 23–34.
13 X. H. Huang and R. N. Zare, *J. Chromatogr., A*, 1990, **516**, 185–189.
14 X. H. Huang and R. N. Zare, *Anal. Chem.*, 1990, **62**, 443–446.
15 Y.-F. Cheng, M. Fuchs, D. Andrews and W. Carson, *J. Chromatogr., A*, 1992, **608**, 109–116.
16 K. O. Eriksson, A. Palm and S. Hjerten, *Anal. Biochem.*, 1992, **201**, 211–215.
17 M. Minarik, K. Klepárník, M. Gilár, F. Foret, A. W. Miller, Z. Sosic and B. L. Karger, *Electrophoresis*, 2002, **23**, 35–42.
18 O. Muller, F. Foret and B. L. Karger, *Anal. Chem.*, 1995, **67**, 2974–2980.
19 T. Irie, T. Oshida, H. Hasegawa, Y. Matsuoka, T. Li, Y. Oya, T. Tanaka, G. Tsujimoto and H. Kambara, *Electrophoresis*, 2000, **21**, 367–374.
20 M. Minarik, F. Foret and B. L. Karger, *Electrophoresis*, 2000, **21**, 247–254.
21 K. D. Altria and Y. K. Dave, *J. Chromatogr., A*, 1993, **633**, 221–225.
22 A. Manz, N. Graber and H. M. Widmer, *Sens. Actuators, B*, 1990, **1**, 244–248.
23 A. Manz, Y. Miyahara, J. Miura, Y. Watanabe, H. Miyagi and K. Sato, *Sens. Actuators, B*, 1990, **1**, 249–255.
24 A. Manz, D. J. Harrison, E. M. J. Verpoorte, J. C. Fettinger, A. Paulus, H. Ludi and H. M. Widmer, *J. Chromatogr., A*, 1992, **593**, 253–258.
25 D. J. Harrison, A. Manz, Z. H. Fan, H. Ludi and H. M. Widmer, *Anal. Chem.*, 1992, **64**, 1926–1932.
26 S. H. Lee, S. I. Cho, C. S. Lee, B. G. Kim and Y. K. Kim, *Sens Actuators, B*, 2005, **110**, 164–173.
27 D. Belder, M. Ludwig, L. W. Wang and M. T. Reetz, *Angew. Chem., Int. Ed.*, 2006, **45**, 2463–2466.
28 S. J. Haswell, *Nature*, 2006, **441**, 705–705.
29 C. S. Effenhauser, A. Manz and H. M. Widmer, *Anal. Chem.*, 1995, **67**, 2284–2287.
30 J. Khandurina, T. Chovan and A. Guttman, *Anal. Chem.*, 2002, **74**, 1737–1740.
31 R. Lin, D. T. Burke and M. A. Burns, *J. Chromatogr., A*, 2003, **1010**, 255–268.
32 R. Lin, D. T. Burke and M. A. Burns, *Anal. Chem.*, 2005, **77**, 4338–4347.
33 J. J. Tulock, M. A. Shannon, P. W. Bohn and J. V. Sweedler, *Anal. Chem.*, 2004, **76**, 6419–6425.
34 M. A. Strausbauch and P. J. Wettstein, in *Handbook of capillary electrophoresis*, ed. J. P. Landers, CRC Press, 1997, pp. 841-864.
35 A. T. Woolley and R. A. Mathies, *Anal. Chem.*, 1995, **67**, 3676–3680.
36 M. Miyashita, J. M. Presley, B. A. Buchholz, K. S. Lam, Y. M. Lee, J. S. Vogel and B. D. Hammock, *Proc. Natl. Acad. Sci. U. S. A.*, 2001, **98**, 4403–4408.
37 W. Chen, X. Yin, J. Mu and Y. Yin, *Chem. Commun.*, 2007, 2488–2490.
38 P. S. Dittrich and A. Manz, *Nat. Rev. Drug Discov.*, 2006, **5**, 210–218.
39 R. Bharadwaj, J. G. Santiago and B. Mohammadi, *Electrophoresis*, 2002, **23**, 2729–2744.
40 H. Wensink, H. V. Jansen, J. W. Berenschot and M. C. Elwenspoek, *J. Micromech. Microeng.*, 2000, **10**, 175–180.
41 E. X. Vrouwe, R. Luttge, W. Olthuis and A. van den Berg, *Electrophoresis*, 2005, **26**, 3032–3042.